SURFACE MORPHOLOGY AND OPTICAL AND ELECTROPHYSICAL PROPERTIES OF $La_{0.4}Ba_{0.6}CoO_3$ FILMS OBTAINED BY LASER DEPOSITION

N. A. Bosak,[a,*] A. N. Chumakov,[a] M. V. Bushinsky,[b]
G. M. Chobot,[c] L. V. Baran,[d] A. A. Shevchenok,[c,f]
V. V. Malyutina-Bronskaya,[e] and A. A. Ivanov[a]

UDC 621.373.826:533.9+537.9

Nanostructured thin films on a silicon substrate were obtained by high-frequency repetitively pulsed (f ~ 10–15 kHz) laser action with a wavelength of 1.064 μm and a power density q = 54 MW/cm^2 on $La_{0.4}Ba_{0.6}CoO_3$ ceramics at a vacuum chamber pressure p = 2.2 Pa. The morphology of the obtained films was studied using atomic-force microscopy. Features of transmission spectra in the visible, near-, and mid-IR regions were revealed. The electrophysical properties of the $La_{0.4}Ba_{0.6}CoO_3$ structure were analyzed.

Keywords: *high-frequency laser irradiation, structure of thin films, transmission and reflection spectra, electrophysical characteristics.*

Introduction. Rare-earth cobaltites with the perovskite structure substituted by alkaline-earth ions are promising for various technological applications, particularly in hydrogen energetics, or as thermoelectric materials because of their unique magnetic, electron-transport, and optical properties [1]. They attract attention because of phase transitions associated with a change of spin state of Co^{3+} ions and a correlation of the magnetic and electron-transport properties [1].

As a rule, the magnetic and electrical properties of metallic cobaltites are explained by fundamental mechanisms of magnetic interactions such as a superexchange model, double exchange, and magnetism of collectivized electrons. Each of these mechanisms describes several physical properties of cobaltites. However, it is not universal. Starting $LaCoO_3$ is known to be a diamagnetic dielectric at low temperatures (T < 30 K) [1] while an epitaxial film of $LaCoO_3$ grown on a $(LaAlO_3)_{0.3}(Sr_2AlTaO_6)_{0.7}$ substrate exhibited ferromagnetic ordering below critical temperature $T_c \approx 85$ K [2]. Polycrystalline films of $LaCoO_3$ prepared in the same manner did not exhibit ferromagnetic ordering up to T = 5 K while their temperature-dependent susceptibility was identical to bulk $LaCoO_3$.

The magnetic properties of a thin film of $LaCoO_3$ on Si that was prepared by molecular-beam epitaxy were studied [3]. An x-ray structure analysis was also performed. Thin films of $LaCoO_3$ were prepared by vacuum laser deposition [4]. Their morphological and x-ray structural characteristics were studied. Thin films of double cobaltates with the perovskite structure were of practical interest [5].

The crystal structure and magnetic and electrical properties of ceramic samples of $La_{1-x}Ba_xCoO_{3-\delta}$ solid solutions ($0.5 \le x \le 0.6$) were previously studied [6, 7]. A second-order phase transition and close magnetic ordering related to competitive interaction between two ferromagnetic and antiferromagnetic phases because of the coexistence of Co^{3+} and Co^{4+} were observed in the $La_{1-x}Ba_xCoO_3$ (x = 0.2–0.5) system produced using a high-temperature solid-state reaction in air [8, 9]. However, thin nanostructured films of the $La_{1-x}Ba_xCoO_3$ system are little studied. The unusual physical properties of doped cobaltites, e.g., magnetoresistance [10] and high ionic conductivity [11], make them highly promising for potential use as novel electronic materials for fuel cells, oxygen membranes, and catalysts of chemical reactions for

[*]To whom correspondence should be addressed.

[a]B. I. Stepanov Institute of Physics, National Academy of Sciences of Belarus, Minsk, Belarus; email: n.bosak@ifanbel.bas-net.by; [b]Scientific-Practical Materials Research Center, National Academy of Sciences of Belarus, Minsk, Belarus; [c]Belarusian State Agrarian Technical University, Minsk, Belarus; [d]Belarusian State University, Minsk, Belarus; [e]SSPA Optics, Optoelectronics, and Laser Technology, Minsk, Belarus; [f]Belarusian National Technical University, Minsk, Belarus.

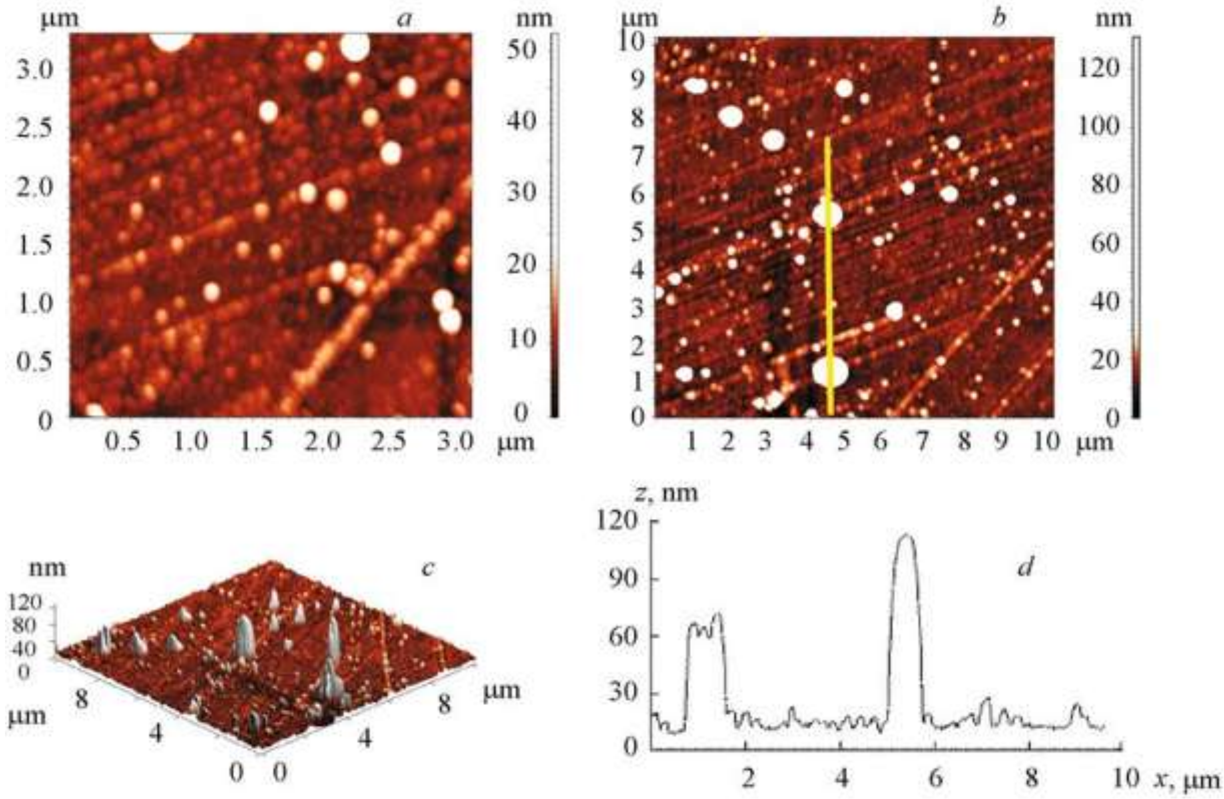

Fig. 1. Surface morphology (a–c) and cross-section profile (d) along the isolated line of a laser-deposited $La_{0.4}Ba_{0.6}CoO_3$ thin film on silicon substrate.

recycling hazardous industrial wastes. Layered oxygen-deficient complex cobalt oxides could find applications in magnetic recording devices [12, 13].

The present work was aimed at studying the properties of nanostructured thin films of $La_{0.4}Ba_{0.6}CoO_3$ on silicon substrate that were formed by multi-pulse high-frequency laser action on a target; investigating the morphology of the obtained thin films using atomic-force microscopy; revealing features of transmission spectra in the near- and mid-IR regions and reflection spectra in the visible and near-IR regions; and measuring the voltammetric (VAC) and volt–Faraday characteristics (VFC).

Experimental. Targets were prepared from a polycrystalline sample of $La_{0.4}Ba_{0.6}CoO_{3-\delta}$ obtained via solid-state reactions in air. The starting reagents were high-purity La_2O_3, $BaCO_3$, and Co_3O_4 taken in the stoichiometric ratio and mixed in a PM-100 planetary ball mill (Retsch). Samples were preliminarily synthesized at 1000°C. $La_{0.4}Ba_{0.6}CoO_{3-\delta}$ was finally synthesized at 1200°C for 14 h. Then, the samples were cooled at 100°C/h to room temperature. An x-ray structural analysis (XSA) of the obtained ceramic at room temperature on a DRON-3M diffractometer using CuK_α-radiation detected no extraneous phases.

$La_{0.4}Ba_{0.6}CoO_3$ films were deposited by high-frequency laser sputtering [14] of the oxide ceramic *in vacuo* (p = 2.2 Pa). The experimental laser system (λ = 1.06 μm) with the laser-pulse repetition rate regulated from 5 to 50 kHz contained a source of laser radiation, an optical system for transporting the laser radiation to the target being sputtered, a vacuum chamber, and a measurement and diagnostic module. The laser-pulse repetition rate was varied by varying the laser pumping level and the optical density of the gate from an irradiated lithium fluoride crystal LiF with F_2^- color centers. The laser pulse length at half-height was τ ~ 85 ns. Macroscopically homogeneous thin films were deposited at laser radiation power density q = 54 MW/cm^2 and pulse repetition rate f ~ 8–10 kHz.

Microscopy studies used an SEM EVO 10 scanning electron microscope with an Oxford Instruments Nanotechnology Tools Ltd. micro-x-ray spectral analyzer. The surface morphology of the samples was studied using a Solver P47-Pro scanning probe microscope (NT-MDT, Russia) in semi-contact mode. Standard Si probes with point radius of curvature

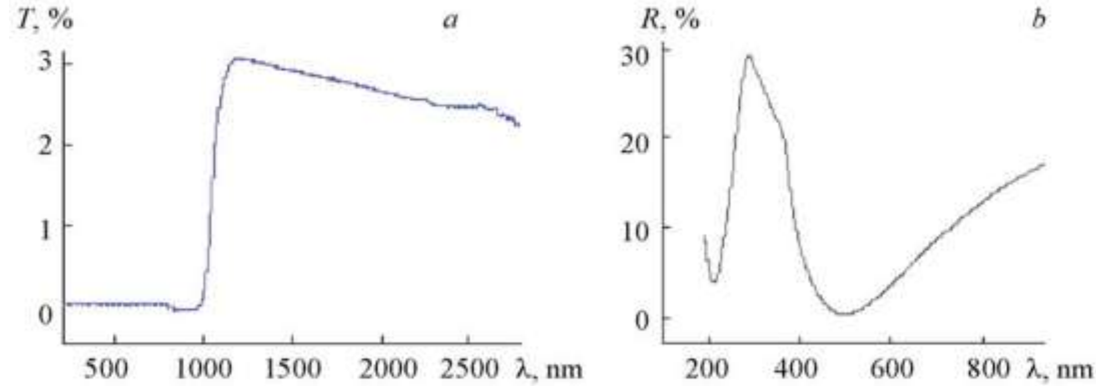

Fig. 2. Transmission (a) and reflection spectra (b) of laser-deposited $La_{0.4}Ba_{0.6}CoO_3$ film on silicon substrate in visible and near-IR regions.

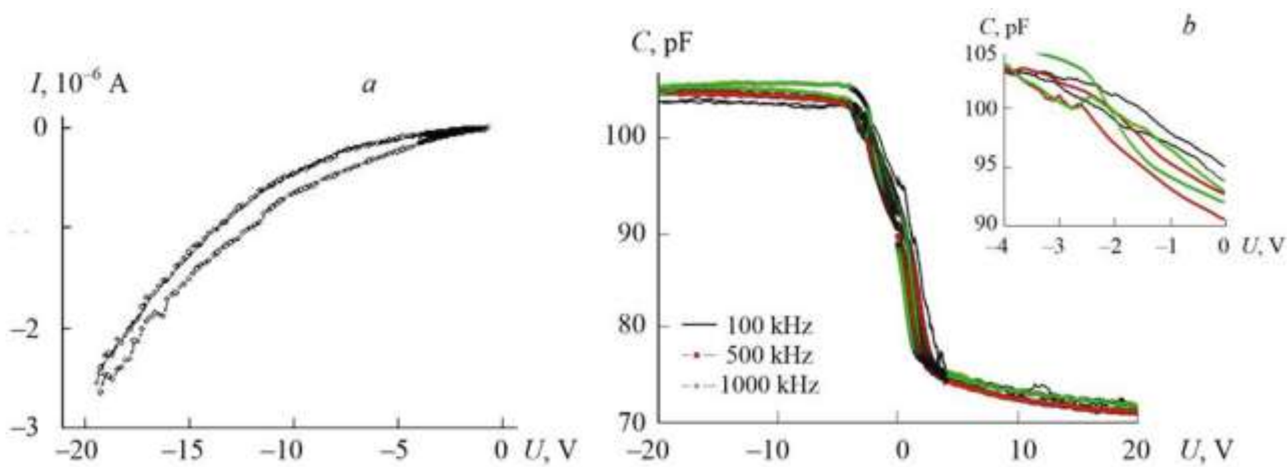

Fig. 3. Voltammetric (a) and volt–Faraday (b) characteristics of $La_{0.4}Ba_{0.6}CoO_3$ thin film on silicon substrate.

< 10 nm were used. Transmission of optical radiation by the thin films in the near-IR region was measured on a Cary 500 Scan spectrophotometer. Transmission spectra in the mid-IR region were recorded using a NEXUS FTIR spectrometer (Thermo Nicolet) in the range 400–4000 cm^{-1}. VAC and VFC were measured using an E7-20 automated immitance meter at room temperature. VFC were measured at signal frequencies 100, 500, and 1000 kHz.

Results and Discussion. According to energy dispersive x-ray microanalysis, $La_{0.4}Ba_{0.6}CoO_3$ film contained all elements present in the sputtered sample. The average contents of La, Ba, and Co in it agreed with their contents in the starting target.

Atomic-force microscopy found that a nanocrystalline structure of $La_{0.4}Ba_{0.6}CoO_3$ thin films formed upon deposition on the Si substrate (Fig. 1a). The average lateral size of the structural elements was 60 nm. The mean-square roughness was ≤6.7 nm. An insignificant number of large particles with lateral size 300–700 nm and height 60–120 nm was observed on the surface (Fig. 1b–d). The average height of the film relief determined at five different sample points not containing these particles scanned over an area of 5 × 5 μm was ≤8 nm. The mean-square roughness was 3.6 nm.

The use of nanosecond laser radiation at various wavelengths seemed like a promising method for producing nanoparticles of various sizes [15].

The transmission of the laser-deposited film of $La_{0.4}Ba_{0.6}CoO_3$ on the Si substrate in the near-IR region (Fig. 2a) dropped from 3.1% for λ = 1214 nm to 2.5% for λ = 2400 nm. The reflection coefficient R of $La_{0.4}Ba_{0.6}CoO_3$ film

(Fig. 2b) decreased in the range 288–495 nm, reaching a minimum of R_{min} = 0.31%. The reflection coefficient began to grow smoothly from λ = 510 nm and reached a maximum of R_{max} = 20.5% at λ = 1100 nm.

Figure 3 shows the VAC and VFC for a $La_{0.4}Ba_{0.6}CoO_3$ thin film on a Si substrate. The current flowing with a positive potential applied to the film was less than the measurement limit of the instrument (not shown). Two sections in the VAC that obeyed a power dependence of the current on potential (characteristic for current limited by space charge in an oxide film with deep traps) could be seen with a negative potential applied to the film (Fig. 3a): $I \sim U^{m}$, where m = 1.83 from –1 to –6 V and m = 2.6 from –6 to –16 V. The VFC were measured at frequencies 100, 500, and 1000 kHz (Fig. 3b). The VFC of the studied system appeared characteristic for an MOS structure. The capacitance of the dielectric at negative potentials and the capacitance of the whole structure did not change with the frequency of the variable potential because minor charge carriers could not accumulate with the potential changing at rather high frequencies.

Maxima in the dependence of the signal frequency were also observed for capacitance modulation from 0 to –4 V (Fig. 3b, inset). The positions of the maxima relative to the potential shift also differed. This indicated that mono-energetic surface states (deep traps) lying at different levels in the bandgap contributed to the capacitance at different frequencies. These surface states were caused by the crystalline oxide film structure and the $La_{0.4}Ba_{0.6}CoO_3$/Si interface.

Conclusions. Nanocrystalline $La_{0.4}Ba_{0.6}CoO_3$ thin films on Si substrate with an average lateral size of the structural elements of 60 nm and a mean-square roughness of 6.7 nm were prepared by high-frequency laser sputtering. The transmission of a $La_{0.4}Ba_{0.6}CoO_3$ film in the near-IR region decreased from 3.1% at a wavelength of 1214 nm to 2.5% at λ = 2400 nm. The reflection coefficient of the film decreased in the range 288–495 nm, reaching a minimum of 0.31%. The electrical properties of the studied film on Si substrate were caused by mono-energetic surface states lying at different levels in the bandgap. These surface states were caused by the crystalline oxide film structure and the $La_{0.4}Ba_{0.6}CoO_3$/Si interface.

REFERENCES

1. N. B. Ivanova, S. G. Ovchinnikov, M. M. Korshunov, I. M. Eremin, and N. I. Kazak, *Usp. Fiz. Nauk,* **179**, 837 (2009).
2. D. Fuchs, C. Pinta, T. Schwarz, P. Schweiss, P. Nagel, S. Schuppler, R. Schneider, M. Merz, G. Roth, and H. V. Lohneysen, *Phys. Rev. B: Condens. Matter Mater. Phys.*, **75**, Article ID 144402 (2007).
3. A. Posadas, M. Berg, H. Seo, A. de Lozanne, A. A. Demkov, D. Smith, A. P. Kirk, D. Zhernokletov, and R. M. Wallace, *Appl. Phys. Lett.*, **98**, Article ID 053104 (2011).
4. M. Jedrusik, L. Cieniek, A. Kopia, Ch. Turquat, and Ch. Leroux, *Arch. Metallurgy Mater.*, **65**, No. 2, 793–797 (2020).
5. M. Liu, S. P. Ren, R. Y. Zhang, Z. Y. Xue, C. R. Ma, M. L. Yin, X. Xu, S. Y. Bao, and C. L. Chen, *Sci. Rep.*, **5**, Article ID 10784 (2015).
6. I. O. Troyanchuk, M. V. Bushinsky, A. V. Nikitin, L. S. Lobanovsky, A. M. Balagurov, V. Sikolenko, V. Efimov, and D. V. Sheptyakov, *J. Appl. Phys.*, **113**, Article ID 053909 (2013).
7. I. O. Troyanchuk, M. V. Bushinsky, N. Tereshko, C. Ritter, V. Sikolenko, and M. Silibin, *Phys. Status Solidi B*, **255**, No. 10, Article ID 1800315 (2018).
8. T. L. Phan, T. V. Manh, H. R. Park, B. W. Lee, S. C. Yu, H. Yang, C. Li, H.-G. Piao, Y. D. Zhang, D. H. Manh, and N. T. Dang, *J. Magn. Magn. Mater.*, **539**, Article ID 168378 (2021).
9. T. L. Phan, D. N. Petrov, J. Cwik, N. T. Dang, and V. Dongquoc, *Curr. Appl. Phys.*, **18**, No. 11, 1248–1254 (2018).
10. T. Saitoh, T. Mizokawa, A. Fujimori, M. Abbate, Y. Takeda, and M. Takano, *Phys. Rev. B: Condens. Matter Mater. Phys.*, **55**, Article ID 4257 (1997).
11. A. Mineshige, M. Inaba, T. Yao, Z. Ogumi, K. Kikuchi, and M. Kawase, *J. Solid State Chem.*, **121**, 423 (1996).
12. B. Raveau and M. Seikh, *Cobalt Oxides, from Crystal Chemistry to Physics*, Wiley-VCH (2012).
13. S. Mitrovski and D. M. Drazic, *J. Serb. Chem. Soc.*, **65**, No. 7, 555–564 (1998).
14. L. Ya. Min′ko, A. N. Chumakov, and N. A. Bosak, *Kvantovaya Élektron. (Moscow)*, **17**, No. 11, 1480–1484 (1990).
15. A. V. Butsen′ and N. V. Tarasenko, *Kvantovaya Élektron. (Moscow)*, **40**, No. 11, 986–1003 (2010).